sciendo

Ornis Hungarica 2022. 30(2): 45–60.
DOI: 10.2478/orhu-2022-0019

Allometric inter-relationships between jaw musculature mass, skull size and body mass in *Psittaciformes*

Shannon L. Harrison, Gregory P. Sutton & D. Charles Deeming*

Received: July 07, 2022 – Revised: August 10, 2022 – Accepted: August 13, 2022

Harrison, S. L., Sutton, G. P. & Deeming, D. C. 2022. Allometric inter-relationships between jaw musculature mass, skull size and body mass in *Psittaciformes*. – Ornis Hungarica 30(2): 45–60. DOI: 10.2478/orhu-2022-0019

Abstract Functional characteristics of the jaw apparatus, for example bite force, in vertebrates is a combination of the skeleton and the musculature. In birds, bite force has been measured directly or calculated using various methods including summation of forces generated by the different elements of the jaw musculature. However, there have been no reports of the relationships between body size with the mass of the different muscle groups in a closely related group of birds. This study explored allometry in the different jaw muscle masses from parrot (Psittaciformes) species differing in body mass by 40-fold. It was hypothesised that the different muscle masses would exhibit isometry with body mass and skull size. Parrot heads were dissected and the masses of the individual muscle complexes were recorded. Data were subjected to phylogenetically-controlled regression analysis to document scaling effects with body mass and skull size. Most, but not all muscles, exhibited positive allometry with body mass but most were isometric with skull size. Consequently, as parrots get bigger, their skulls get proportionally longer, but that the muscles within the head isometrically scaled relative to the size of these proportionally larger skulls. The large muscles imply greater bite forces in parrots than have been reported to date, which seems to be associated with an increase in skull size to accommodate more muscles. It is unknown whether this pattern is applicable to other birds within specific orders or even across birds as a whole. There needs to be further investigation into the allometry of the morphological and functional properties of the avian jaw musculature.

Keywords: parrot, anatomy, jaw, jaw muscles, skull, skull size, allometry, bite force

Összefoglalás Az állkapocs funkcionális jellemzői, mint például a harapási erő, a gerinceseknél a csontváz és az izomzat kombinációjából adódnak. Madaraknál a harapási erőt közvetlenül mérték vagy különféle módszerekkel számították ki, beleértve az állkapocs izomzatának különböző elemei által generált erők együttesét is. Ennek ellenére nem készültek kutatások a testméret és a különböző izomcsoportok tömege közötti összefüggésekről közeli rokon madárcsoportok esetében. Ez a tanulmány az állkapocs izmok tömegének allometriáját vizsgálta papagájoknál (Psittaciformes), mely csoportban a testtömegbeli különbség akár 40-szeres is lehet a fajok között. A kiindulási hipotézis az volt, hogy a különböző izmok tömegei izometriát mutatnak a testtömeggel és a koponyamérettel. A papagájfejek boncolása után az egyes izomcsoportok tömegét mértük. Az adatokat filogenetikai elemzésnek vetettük alá, hogy megvizsgáljuk a méretkülönbségből adódó hatásokat a testtömeggel és a koponyamérettel kapcsolatban. A legtöbb (azonban nem az összes) izomcsoport pozitív allometriát mutatott a testtömeggel, de a legtöbb izometrikus volt a koponya méretével. Következésképpen, minél nagyobb az adott papagáj testtömege, koponyája arányosan hosszabb, de a fej izmai izometrikusan arányosan nagyobbak a koponyákhoz mérten. A nagyobb izmok nagyobb harapási erőt jelentenek, mint ahogyan azt korábban feltételezték, ami arra enged következtetni, hogy a koponyaméret növekedésével több izomnak biztosítható tapadási felület. Nem ismert, hogy ez a minta alkalmazható-e a madarak más rendjein belül, vagy akár a madarak egészére. További vizsgálatokra van szükség a madarak állkapocs izomzatának morfológiai és funkcionális tulajdonságainak allometriáját illetően.

Kulcsszavak: papagáj, anatómia, állkapocs, állkapocs izmok, koponya, koponyaméret, allometria, harapás erősség

Department of Life Sciences, School of Life and Environmental Sciences, University of Lincoln, Joseph Banks Laboratories, Lincoln, LN6 7DL, UK;
** corresponding author, e-mail: cdeeming@lincoln.ac.uk*

Introduction

Jaw function and associated bite force are important for animals because they determine the range of dietary items an organism can consume (Nogueira *et al.* 2009, Maestri *et al*. 2016, Sakamoto 2021). The anatomy of the jaw apparatus of birds is commonly reported but often only as a qualitative description of the anatomy of the jaw (e.g. Burton 1974a). Other studies have taken a quantitative approach and report the size of the muscles jaw apparatus (e.g. Burger 1978), whereas other studies have a more functional approach exploring bite force, which is an ecologically relevant performance trait (Deeming *et al*. 2022). Bite force is a function of the force exerted by muscle contraction applied via the skeleton. It is often measured *in vivo* with animals biting down on force transducers (Herrel *et al*. 1999, Sustaita & Hertel 2010, Verma *et al*. 2017) but can also be calculated from the morphometrics of skulls (Anderson *et al*. 2008), or using finite element analysis of 3D images generated by computerised tomography (e.g. Cost *et al.* 2020). In addition, skulls can be dissected to reveal muscle masses, which can be used to calculate bite force in birds (Sustaita 2008, Soons *et al*. 2015). Recently, Deeming *et al.* (2022) showed that the relationship between muscle mass and bite force in birds exhibited positive allometry but in reptiles this relationship was isometric (Deeming 2022). Although this difference may reflect taxonomic variability, one possible reason for this discrepancy could be the limited and biased range of species represented in the avian dataset compared to that for reptiles. Deeming (2022) had values for over 275 species of reptile but for birds, 46 of the 122 species were from the Passeriformes and were no larger than 70 g (Deeming *et al*. 2022).

Muscle dissection is a way of calculating bite force, but muscle masses in birds are only reported in a relatively few species, including (but not exclusively): cormorants Suliformes, (Burger 1978), birds of prey Accipitriformes and Falconiformes (Sustaita 2008 and see Hull 1991, 1993, Wang *et al.* 2017, Deeming *et al.* 2022), waterfowl Anseriformes, (Goodman & Fisher 1962), and songbirds Passeriformes, (e.g. van der Meij & Bout 2004). However, within these taxa the spread of data can be limited. For instance, data for muscle mass is available from only 7 different families of songbirds (see Deeming *et al*. 2022) and often these data represent values for all jaw muscles combined. However, the jaw musculature of birds is a complex of different muscle groups, which all have differing roles in the operation of the jaw (Burger 1978, Bhattacharyya 2013): depressors (that open the jaw); adductors (that raise the mandible); protractors (which lower the upper jaw); and retractors (which simultaneously raise the mandible and lower the upper jaw). In passerines, data for masses of these different muscle groups are limited to 10 species from two bird families, which only vary in body mass between 9–33 g (Soons *et al*. 2012, 2015). However, even across a limited size range van der Meij and Bout (2004) showed that total jaw muscle mass, and individual functional muscle groups, exhibited positive allometry with body mass in the Fringillidae and Estrildidae. This paucity of data, and limited ranges in body size for

muscle masses in birds, leave little scope for exploring allometric scaling relationships for different jaw muscle types and how these could impact on the functional properties of the jaw apparatus, that is bite force.

The Psittaciformes are noted for their strong bite force (Carril *et al.* 2015, Cost *et al.* 2020) and dexterity in processing food items with the beak (Auersperg *et al.* 2012, Toft & Wright 2015). Body masses (Dunning 2008) in parrots range from around 12 g for pygmy-parrots (*Micropsitta* spp.) through to over 1300 g for the Hyacinth Macaw *(Andorhynchus hyacinthinus)* for 2000 g for the male, flightless Kakapo *(Strigops habroptila)*. This range of body sizes offers scope to investigate the relationships between body size with the mass of the different muscle groups in a closely related group of birds. This study, therefore, explored allometry in the different jaw muscle masses from a variety of parrot species ranging in body mass by 40-fold. Given the similarity in skull and beak morphology seen in the Psittaciformes (Zusi 1993), because earlier studies in reptiles showed that muscle mass isometrically scaled with body mass and showed marginal positive allometry with skull size (Deeming 2022), we hypothesized that this would also be true in Psittaciformes. The results will provide an insight into how body size impacts on the myology of the jaw apparatus in this order and how this may impact on the functional properties of the jaw apparatus, i.e. the production of bite force.

Methods

Parrot cadavers of nineteen species were obtained from the Lincolnshire Wildlife Park, Friskney, Lincolnshire, UK. All birds had died of natural causes and sample sizes varied according to species *(Table 1)*. The birds were stored in plastic bags and frozen at –20 ºC until required. The cadavers were often not intact and so body mass (in g) used for the parrots was the average reported by Dunning (2008) rather than the mass of the bird at the time of dissection. The range of body masses *(Table 1)* was from 29 g for the Budgerigar *(Melopsittacus undulatus)* to 1215 g for the Red-and-green Macaw *(Ara chloropterus)*.

Birds were defrosted for 24 hours prior to dissection. The heads of the parrots were cut from the bodies before being skinned, exposing the muscles. Each muscle complex was identified and dissected away from the skull. Subdivisions of the muscles (Homberger 2017) were not considered because the contraction of the elements of a muscle complex would have the same physical effect. Muscle tissue was then blotted dry and the wet mass recorded (in g) using a digital Sartorius® micro balance. Where possible, both sides of the head were dissected but in some specimens the muscles were damaged, so data were only available from one side. Therefore, data are presented as an average muscle mass of one side of the head.

To expose the skull for measurement, the head was de-fleshed by soaking in Tergazyme at 15% concentration at 40 ºC. The skulls were then soaked in a solution of concentrated washing up liquid and water, to remove any Tergazyme residue and any residual grease from the bones before drying for 2–3 days in an incubator at 20 ºC. Using digital callipers (RS Pro, 2020), the total length of skull was measured (in mm) from a dorsal view and was the distance between the supraoccipital crest and the tip of the maxilla.

Table 1. Mean (± SE) body mass (in g, as reported by Dunning, 2008), skull length (in mm), and masses of individual single muscle complexes (in g) per species. Number of individuals in the dataset are indicated in parenthesis. Standard error values were calculated for species values where there were 3 or more individuals present

1. táblázat Átlagos (± SE) testtömeg (g-ban, Dunning, 2008 után), koponyahossz (mm) és az egyes izomcsoportok tömege (g) fajonként megadva. A vizsgálatban szereplő egyedek száma a zárójelben van feltüntetve. A sztenderd hibaértékeket azokra a fajokra számítottuk, ahol 3 vagy annál több egyed szerepelt

Species	Body mass (g)	Skull length (mm)	*Depressor mandibulae* (g)	*Adductor mandibulae externus* (g)	*Pseudomasseter* (g)	*Pterygoideus ventralis* (g)	*Pterygoideus dorsalis* (g)	*Ethmomandibularis* (g)
Cacatua alba (N = 3)	570.0	78.0 ± 2.2	1.00 ± 0.12	0.70 ± 0.08	0.99 ± 0.43	1.71 ± 0.22	0.69 ± 0.04	0.68 ± 0.09
Cacatua galerita (N = 3)	720.4	76.9	1.22	0.91	1.39	2.32	0.74	1.49
Cacatua moluccensis (N = 1)	835.0	91.3	1.10	0.89	1.65	2.19	0.95	0.97
Melopsittacus undulatus (N = 1)	29.0	27.3	0.03	0.01	0.01	0.02	0.01	0.02
Psittacula eupatria (N = 1)	214.0	59.0	0.42	0.25	0.64	1.05	0.30	0.43
Psittacula krameri (N = 4)	116.1	45.8 ± 0.9	0.10 ± 0.02	0.07 ± 0.01	0.10 ± 0.01	0.24 ± 0.02	0.08 ± 0.01	0.17 ± 0.01
Ara ararauna (N = 3)	1125.0	106.4 ± 5.3	1.27 ± 0.06	1.02 ± 0.07	0.63 ± 0.25	2.31 ± 0.17	1.30 ± 0.14	1.81 ± 0.61
Ara chloropterus (N = 3)	1214.0	117.8 ± 1.5	2.07 ± 0.20	1.98 ± 0.41	0.44 ± 0.12	4.99 ± 0.71	2.33 ± 0.23	2.04 ± 0.58
Ara macao (N = 1)	1015.0	103.9	1.26	1.30	0.37	2.94	1.13	0.81
Amazona aestiva (N = 2)	451.0	65.6	0.35	0.18	0.31	0.62	0.25	0.43
Amazona amazonica (N = 3)	370.0	67.6 ± 2.0	0.34 ± 0.04	0.20 ± 0.01	0.30 ± 0.02	0.76 ± 0.10	0.21 ± 0.02	0.36 ± 0.03
Amazona auropalliata (N = 1)	476.9	65.6	0.32	0.28	0.61	0.79	0.22	0.47
Amazona autumnalis (N = 2)	416.0	72.2	0.31	0.19	0.46	0.77	0.25	0.35
Amazona farinosa (N = 1)	626.0	79.8	0.51	0.25	0.38	1.21	0.52	0.95
Amazona ochrocephala (N = 3)	476.9	65.3 ± 2.2	0.34 ± 0.01	0.20 ± 0.03	0.28 ± 0.05	0.80 ± 0.10	0.22 ± 0.02	0.58 ± 0.03
Amazona oratrix (N = 1)	517.0	72.4	0.26	0.28	0.18	0.53	0.19	0.29
Myiopsitta monachus (N=3)	120.0	41.8 ± 2.8	0.10 ± 0.02	0.10 ± 0.01	0.05 ± 0.01	0.14 ± 0.02	0.08 ± 0.01	0.11 ± 0.01
Poicephalus senegalus (N = 2)	147.0	49.6	0.10	0.11	0.16	0.33	0.14	0.22
Psittacus erithacus (N = 5)	333.0	71.5 ± 1.8	0.46 ± 0.04	0.52 ± 0.10	0.44 ± 0.09	1.01 ± 0.15	0.25 ± 0.03	0.52 ± 0.09

Mean values were calculated for those species which had repeated samples *(Table 1)*. Unless stated otherwise, mass and linear measurments were $\log_{10}$-transformed prior to analysis and analysis was performed in R (version 4.0.3; R Development Core Team 2021). Linear models were used to compare logit-transformations (Warton & Hui 2011) of the proportions of the different muscles in the three genera where there were three or more representatives, i.e. the macaws *(Ara)*, amazons *(Amazona)* and cockatoos *(Cacatua)*.

Allometric relationships among body mass, skull length and muscle masses were explored using phylogenetically controlled general linear modelling (pglm) performed in R. This analysis used the statistical packages "*ape*" (Paradis *et al*. 2004), "*MVTnorm*" (Genz & Bretz 2009), and "*MASS*" (Venables & Ripley 2002), with additional code supplied by Dr Carl Soulsbury (personal communication) to run the phylogenetically controlled generalised linear models to test for the linear relationship between variables. To control for phylogeny, a time calibrated phylogeny was constructed using a subset downloaded from the Hackett all species backbone birdtree.org (Jetz *et al*. 2012) and was identical to the tree presented by Provost *et al*. (2018). The phylogenetic signal, λ, indicated that the observed covariance in residuals was similar to that expected under a Brownian motion model of trait evolution (Freckleton *et al.* 2002). By contrast, a low value for λ indicated that this relationship exhibited no discernible evolutionary signal (Freckleton *et al*. 2002). Comparison of exponents against expected isometric slopes was performed using one-sample t-tests based on the method of Bailey (1981).

Results

Muscle complexes

Six muscle complexes were identified in the jaw musculature of the parrot species investigated following previous descriptions (Homberger 2003, 2017, Tokita 2003, Carril *et al*. 2015). These are briefly described here in terms of their physical location and characteristics *(Figure 1)*.

Depressor mandibulae (DM, *Figure 1*, grey): The *depressor mandibulae* muscle was the main depressor of the jaw and originated caudal to the occipital region on the skull, running downwards along the occipital crest. The upper portion of the muscle was wider than its insertion. This sheet of muscle inserted onto, and along the posterior edge of, the mandible on the dorsal aspect of the articular.

Adductor mandibulae externus complex (AME, *Figure 1*, red): This was the larger of the three adductor muscle complexes, which consisted of highly integrated muscle sub-divisions. In general, this complex had a large area of origin over the skull associated with the *adductor mandibulae externus superficialis* that originated at the *fossa temporalis* and through the fossa beneath the orbit. In macaws (*Ara* spp.), this muscle covered a large area of bone around the dorsal aspect of the occipital process, whereas in the Budgerigar there was very little external coverage of this muscle. The AME complex then appeared to convert from surface to point attachment whereby a portion of the muscle suspended internally

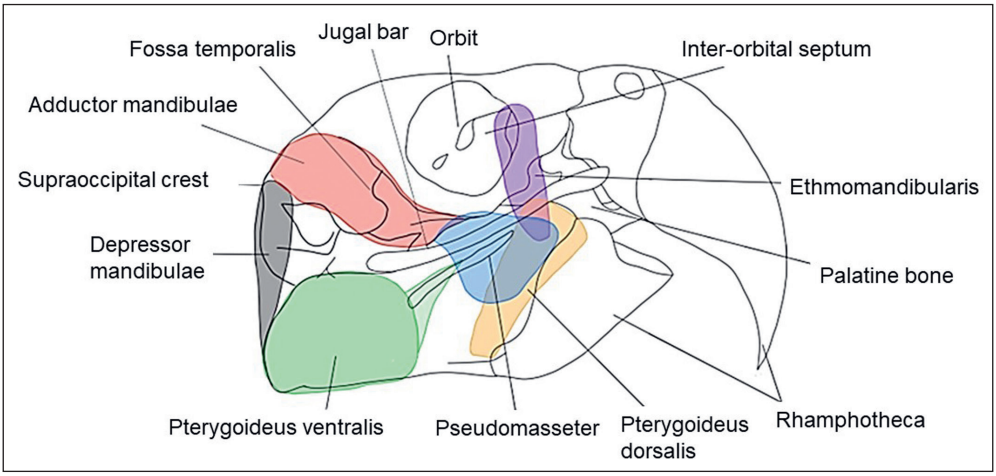

Figure 1. An outline of an *Ara chloropterus* skull with the various jaw muscles illustrated by different colours. See text for more details

1. ábra Egy *Ara chloropterus* koponyájának körvonala az egyes állkapocsizmokkal, különböző színekkel jelölve. További részletek a szövegben

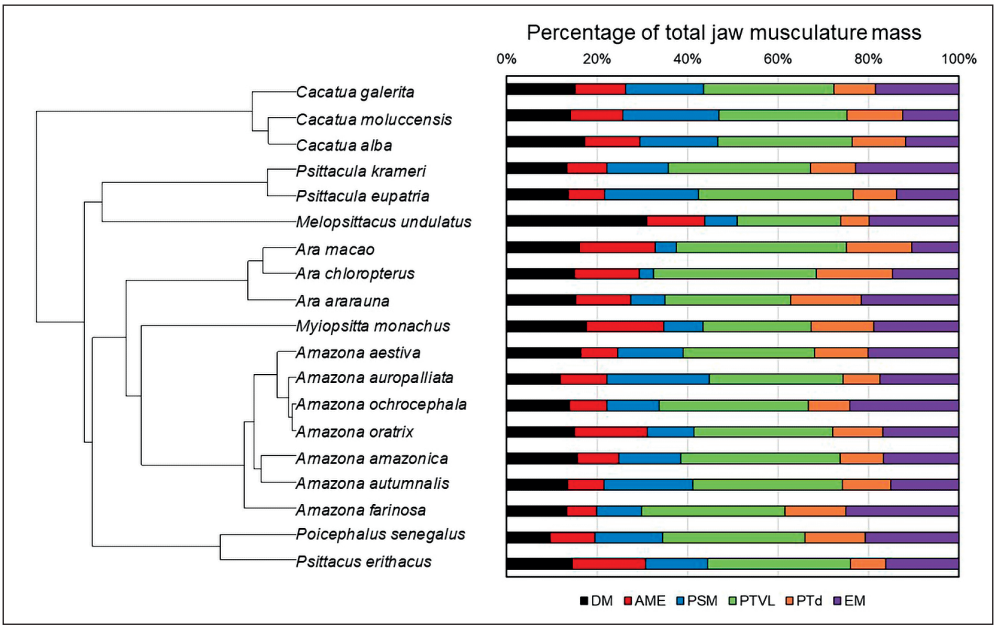

Figure 2. Phylogenetic tree showing the relatedness of the species within this dataset (generated by birdtree.org) alongside each individual muscle mass expressed as a mean percentage of the total muscle mass. DM – *Depressor mandibulae*, AME – *Adductor mandibulae*, PSM – *Pseudomasseter,* PTVL – *Pterygoideus ventralis,* EM – *Ethmomandibularis*, PTd – *Pterygoideus dorsalis*

2. ábra A tanulmányban szereplő fajok filogenetikai viszonya (forrás: birdtree.org), valamint az egyes fajokhoz tartozó átlagos izomtömegek százalékos aránya. DM – *Depressor mandibulae*, AME – *Adductor mandibulae*, PSM = *Pseudomasseter,* PTVL – *Pterygoideus ventralis,* EM – *Ethmomandibularis*, PTd – *Pterygoideus dorsalis*

within the cranium attaching to the lower jaw between two ridges on medial edge of the mandible.

Pseudomasseter (PSM, *Figure 1*, blue): The *pseudomasseter* muscle was a second adductor muscle found on the exterior lateral surface of the skull and mandible, originating from the mid-distal end of the *arcus suborbitalis* seen in some species, especially cockatoos (Cacatuidae). The PSM was a sheet of muscle that attached to the surface of the mandible at the anterior region, extending antero-dorsally outwards both towards the superior and inferior regions of the mandibular rhampotheca. Species of *Ara* and *Psittacula* had undeveloped *pseudomassester* muscles compared with those observed in species of *Cactua* and *Amazona*.

Ethmomandibularis (EM, *Figure 1*, purple): This substantial adductor muscle lacked subdvisions and originated from a large region ventral to the inter-orbital septum and followed downwards the length of the *os ectethmoidale*. The EM inserted onto the inside of the lower mandible towards the cranial aspect of the jaw.

Pterygoideus ventralis (PTVL, *Figure 1*, green): This muscle complex was the largest retractor and was closely associated with the *pterygoideus dorsalis* muscle (see below). However, the *pterygoideus ventralis* was a sheet of muscle predominantly located on the external surface of the mandible. The PTVL originated from the pterygoid bone and then extends downwards to the bottom of the mandible. It then wrapped around the ventral edge of the mandible, eventually inserting on the outer lateral surface of the mandible in a fan-like manner. Superficially this muscle is covered by an aponeurosis. This muscle exhibited some variability not only in mass but in its association with surrounding structures. For example, in the Cacatuidae the PTVL was superficially robust, extending outwards away from the edge of the mandible and closely

Table 2. Results from phylogenetically-corrected linear regression models testing the relationships between average body mass (g), average skull length (mm) and average total jaw muscle mass (g), for 19 species of parrot. All data were $\log_{10}$-transformed before analysis and the intercepts presented at log-values

2. táblázat Az átlagos testtömeg (g), az átlagos koponyahossz (mm) és a teljes állkapocs izomtömegének átlaga (g) közötti összefüggéseket bemutató táblázat, amelyek értékei filogenetikailag korrigált lineáris regressziós modellek eredményei a vizsgálatban szereplő 19 papagájfaj esetében. Az elemzés előtt minden adat 10-es alapú logaritmus értékét vettük, az így kapott tengelymetszetek log-értékeit tüntettük fel

Relationship		Exponent (SE)	t (p-value)	$F_{1,17}$	R^2	λ
Skull length vs Body mass	Intercept Slope	0.832 (0.054) 0.389* (0.020)	15.28 (<0.0001) 19.60 (<0.0001)	384.3	0.957	0.911^{A}
Jaw muscle mass vs Body mass	Intercept Slope	-2.984 (0.278) 1.339** (0.105)	-10.73 (p<0.0001) 12.81 (p<0.0001)	164.1	0.958	$0.676^{A,B}$
Jaw muscle mass vs Skull length	Intercept Slope	-5.577 (0.444) 3.283 (0.242)	-12.56 (p<0.001) 13.60 (p<0.0001)	184.8	0.916	0.241^{B}

Slope values with * and ** indicate significant departures from isometry for skull length against body mass (isometric slope = 0.333), or jaw muscle mass against body mass (isometric slope = 1.0), at P = 0.05 and P = 0.01, respectively. The slopes for jaw muscle mass against skull length did not significantly depart from an isometric slope of 3.0. For λ values, superscript A and B indicate a significant difference from a value of 0 or 1, respectively at least P < 0.05

A *-al és **-al jelölt iránytangens értékek szignifikáns eltéréseket mutatnak az izometriát tekintve a koponyahossznak a testtömeghez (izometrikus meredekség = 0,333), illetve az állkapocs izomtömegének a testtömeghez viszonyítva (izometrikus meredekség = 1,0), P = 0,05 és P = 0,01. Az iránytangensek az állkapocs izomtömegének a koponya hosszához viszonyítva nem mutattak szignifikáns eltérést a 3,0 izometrikus meredekségtől

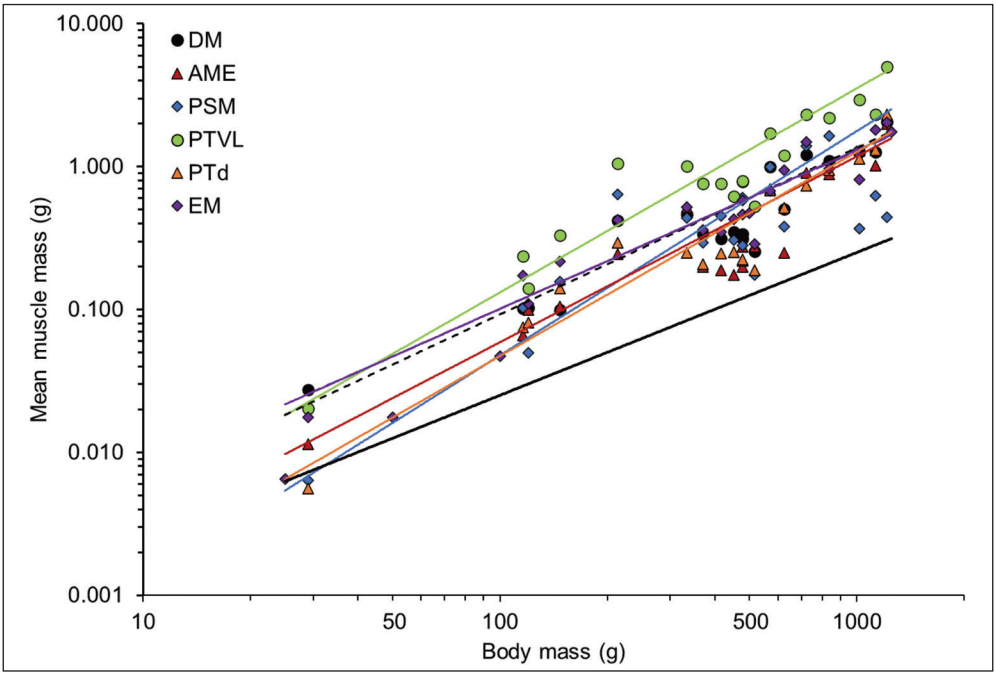

Figure 3. Relationships between mean values for body mass and individual jaw muscle masses for each parrot species. Colour of trendlines equates to the equivalent muscle symbol (except for DM, which is a dashed line), and were generated using phylogenetically controlled linear models calculated in R (see *Table 3*). The solid black line at the bottom is to illustrate a line with a slope of 1.0

3. ábra A testtömeg átlagértékei és az egyes papagájfajok állkapcsát alkotó izmok tömege közötti összefüggés. A trendvonalak színe megegyezik az egyes izmok szimbólumaival (ez alól kivételt képez a DM, ezt szaggatott vonal jelöli), az ábrát R-ben filogenetikailag kontrolált lineáris modellekkel hoztuk létre (lásd a *3. táblázat*). A legalsó folytonos fekete vonal az 1-es meredekséget szemlélteti

aligning with the equally substantial *pseudomasseter* (discussed earlier). In the Budgerigar and the Rose-ringed Parakeet *(Psittacula krameri)* the PTVL was relatively small, with very little definition between the outline of the lower jaw and the muscle itself.

Pterygoideus dorsalis (PTd, *Figure 1*, orange): The *pterygoideus dorsalis* was a substantial retractor muscule that originated from the edge of the dorsal element of the palatine and pterygoid bones and attached along the length of the bone's lateral surface. It inserted onto the mandible, past the quadrate and along a medial ridge which sat below the caudal mandibular fenestra.

The mass of each muscule complex varied between species *(Table 1)* and formed different proportions of the total jaw muscle mass *(Figure 2)*. The PTVL muscle formed the majority (on average 30.8%) of the total muscle mass in the parrots but other muscles varied between taxa. In particular, the PSM formed a significantly higher proportion of the total jaw muscle mass ($F_{2,10} = 15.24$, $P < 0.001$) in cockatoos (*Cactua* sp., 18.6%) and amazons (*Amazona* sp., 14.6%) compared with macaws (*Ara* sp., 5.1%). By contrast, the PTd muscle formed a

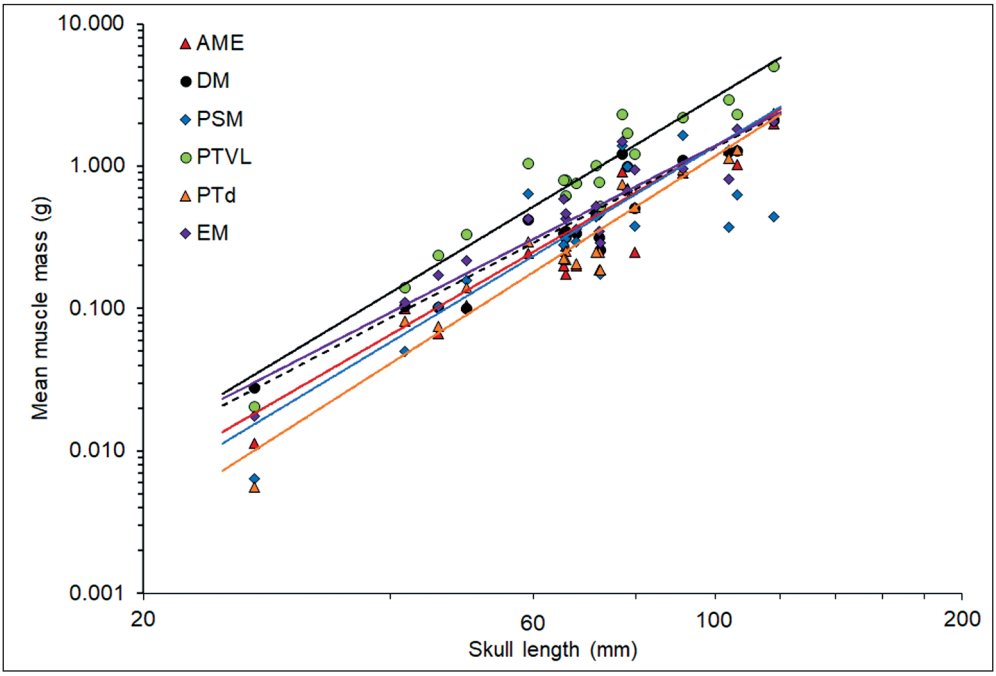

Figure 4. Relationships between mean values for skull length and individual jaw muscle masses for each parrot species. Colour of trendlines equates to the equivalent muscle symbol (except for DM, which is a dashed line), and were generated using phylogenetically controlled linear models calculated in R (see *Table 3*). The solid black line at the bottom is to illustrate a line with a slope of 3.0

4. ábra A koponyahosszok átlagértékei és az egyes papagájfajok állkapcsát alkotó izmok tömege közötti összefüggés. A trendvonalak színe megegyezik az egyes izmok szimbólumaival (ez alól kivételt képez a DM, ezt szaggatott vonal jelöli), az ábrát R-ben filogenetikailag kontrolált lineáris modellekkel hoztuk létre (lásd a *3. táblázat*). A legalsó folytonos fekete vonal a 3-as meredekséget szemlélteti

significantly greater proportion of the total muscle mass in macaws compared to cockatoos and amazons (15.6%, 11.1% and 10.5% respectively; $F_{2,10} = 7.96$, $P < 0.01$). No significant differences were observed between these genera for the other muscle types.

Allometric relationships

There was a highly significant positive relationship between body mass and skull length *(Table 2)*. The phylogenetically-controlled slope was 0.39, which was significantly higher than the predicted isometric slope of 0.33 ($t_{18} = 2.82$, $P = 0.012$) with a high R^2 and high phylogenetic signal *(Table 2)*. Total jaw muscle mass also had highly significant relationships with body mass and skull length, and although the R^2 values were high, the phylogenetic signal was high for body mass but low for skull length *(Table 2)*. Total muscle mass showed significant positive allometry with body mass (observed slope of 1.34, which was significantly different from the hypothesized isometric slope of 1.0; $t_{18} = 3.24$, $P < 0.01$)

Table 3. Results from phylogenetically corrected models testing the effect of the body mass (g) and average skull length (mm) against the average individual muscle masses (g) for 19 species of parrot. All data were log_{10}-transformed before analysis and the intercepts presented at log-values

3. táblázat A filogenetikailag korrigált modellek eredményei, amelyek az átlagos testtömeget (g) és az átlagos koponyahosszat (mm) vizsgálták az egyes egyedek átlagos izomtömegének átlagához mérten (g) 19 papagájfaj esetében. Az elemzés előtt minden adat 10-es alapú logaritmus értékét vettük, az így kapott tengelymetszetek log-értékeit tüntettük fel

		Body mass					Skull length				
Muscle complex		**Exponent (SE)**	**t (p-value)**	**$F_{1,17}$**	**R^2**	**λ**	**Exponent (SE)**	**t (p-value)**	**$F_{1,17}$**	**R^2**	**λ**
Depressor mandibulae (DM)	Intercept Slope	-3.37 (0.27) 1.17 (0.10)	-12.62 (<0.0001) 11.58 (<0.0001)	134.1	0.887	0.591^{A,B}	-5.89 (0.43) 3.01 (0.24)	-13.55 (<0.0001) 12.74 (<0.0001)	162.3	0.905	0.399^{B}
Adductor mandibulae externus (AME)	Intercept Slope	-3.83 (0.34) 1.30* (0.13)	-11.18 (<0.0001) 10.25 (<0.0001)	105.1	0.861	0.829^{A}	-6.48 (0.54) 3.27 (0.29)	-12.00 (<0.0001) 11.15 (<0.0001)	124.4	0.880	0.607
Pseudomasseter (PSM)	Intercept Slope	-4.46 (0.56) 1.57* (0.21)	-7.90 ((<0.0001) 7.55 (<0.0001)	57.0	0.770	0.859	-6.79 (1.03) 3.47 (0.56)	-6.59 ((<0.0001) 6.20 (<0.0001)	38.5	0.693	0.620
Pterygoideus ventralis (PTVL)	Intercept Slope	-3.74 (0.32) 1.43** (0.12)	-11.59 (<0.0001) 11.75 (<0.0001)	137.9	0.890	0.617^{B}	-6.44 (0.46) 3.46 (0.25)	-14.46 (<0.0001) 13.99 (<0.0001)	195.6	0.920	0.053^{B}
Pterygoideus dorsalis (PTd)	Intercept Slope	-4.19 (0.34) 1.43** (0.13)	-12.50 (<0.0001) 11.30 (<0.0001)	127.7	0.883	0.598^{B}	-7.27 (0.47) 3.67* (0.25)	-15.63 (<0.0001) 14.49 (<0.0001)	210.1	0.925	0.012^{B}
Ethmomandibularis (EM)	Intercept Slope	-3.22 (0.25) 1.11 (0.09)	-13.09 (<0.0001) 11.80(<0.0001)	139.3	0.891	0.025	-5.76 (0.48) 2.95 (0.26)	-11.97 (<0.0001) 11.27 (<0.0001)	127.1	0.882	<0.0001^{B}

Slope values with * and ** indicate significant departures from isometry for muscle mass against body mass (isometric slope = 1.0) or skull length (isometric slope = 3.0) at P = 0.05 and P = 0.01, respectively. Slopes for all other relationships did not depart from isometry. For λ values, superscript A and B indicate a significant difference from a value of 0 or 1, respectively at least P < 0.05.

A *-al és **-al jelölt iránytangens értékek szignifikáns eltéréseket mutatnak az izomtömegnek a testtömeghez (izometrikus meredekség = 0,333), illetve a koponyahosszhoz viszonyítva (izometrikus meredekség = 3,0), P = 0,05 és P = 0,01. Az iránytangensek az összes többi összefüggésben nem mutattak szignifikáns eltérést az izometriától.

but the slope for total muscle mass against skull length exhibited an isometic relationship (expected slope of 3.0; $t_{18} = 1.17$, P = 0.196).

All of the relationships between muscle mass type and body mass exhibited significant positive relationships with high values for R^2 *(Figure 3, Table 3)*. The relationships for the *depressor mandibulae* and *ethmomandibularis* were isometric (compared to an expected slope of 1.0) but all of the other muscles exhibited significant positive allometry *(Figure 3, Table 3)*. The phylogenetic signal, λ, was moderate to high for most muscles but by contrast λ was very low for the *ethmomandibularis*, indicating that this relationship exhibited no discernible evolutionary signal.

There were significant positive relationships between the mass of each muscle and skull length *(Figure 4, Table 3)*. These relationships were all isometric (compared to an expected slope of 3.0) with the exception of the *pterygoideus dorsalis*, which exhibited significant positive allometry *(Table 3)*. The phylogenetic signal was relatively low for the *depressor mandibulae* and moderate for the adductor muscles but was very low for each of proractor muscles *(Table 3)*.

Discussion

Contrary to expectations larger parrots had greater total masses of the jaw muscles than smaller parrots and generally each muscle type also exhibited positive allometry with body mass but not skull length. The parrots varied in the relative composition of the muscle in the jaw apparatus with genera varying in their arrangement of the adductor and protractor muscles. Unlike lizards, whose head size scales isometrically with body mass (Deeming 2022), as Psittaciformes get larger, their heads become a proportionally larger part of their body. The jaw muscles, however, scaled isometrically with the size of these proportionally larger heads. Consequently, the high bite forces of the large Psittaciformes is due to them having proportionally larger heads then the smaller Psittaciformes. The muscle geometry within the heads of the Psittaciformes is, however, conserved, with the muscle mass scaling isometrically with the size of the head.

The arrangement of muscle types observed in this study matched that of other studies of the parrot jaw musculature (Burton 1974b, Homberger 2003, 2017, Tokita 2003, Carril *et al.* 2015, Cost *et al*. 2020) although the *protractor pterygoideus et quadrati* reported by Carril *et al.* (2015) was not differentiated here. This may have been because this relatively deep muscle was included with the *pterygoideus dorsalis* or *pterygoideus ventralis* muscles or it was not present, as seemed to be in case in the African Grey Parrot *(Psittacus erithacus)* (Cost *et al*. 2020). The *ethmomandibularis* was found in all species and was a substantial part of the musculature. This muscle has been observed in all parrots examined to date (Burton 1974b, Bühler 1981, Tokita 2003, Carril *et al.* 2015, Homberger 2017, Cost *et al*. 2020) but is not unique to parrots. It was reported in the Hawfinch (*Coccothraustes coccothraustes*, Fringillidae) where it is an adductor muscle (Sims 1955). It is unknown whether this is a feature of other *Coccothraustes* species, or whether other finch species have this muscle, but such possibilities are worthy of further investigation.

Previous reports of the muscles of the parrots the African Grey Parrot (Cost *et al.* 2020) and the Monk Parakeet *(Myiopsitta monachus)* (Carril *et al.* 2015) have values of the jaw muscles that close the jaw (Deeming *et al.* 2022), which are around twice the values recorded in the present study. This may reflect variation between birds or perhaps the published values were for both sides of the jaw combined. Deeming *et al.* (2022) did suggest that there was a lack of clarity in what the published values actually represented and that they were from one side was assumed. It would be more useful if future reports of jaw musculature were explicit in describing what values represent.

The proportions of the adductors and retractors in parrots were approximately equal (on average 0.42 of total muscle mass), which is different to the predominance of the adductors in the Fringillidae and Estrildidae, which form 0.47–0.51 of the total muscle mass compared with 0.34–0.37 for the pterygoid complex (van der Meij & Bout 2004). This may reflect the use of the beak by finches and estrilds to generate high forces to dehusk seeds (van der Meij & Bout 2006). Although bite force has yet to be recorded in the Hawfinch, which has an *ethmomandibularis,* it is anticpated to be high because the similarly sized Yellow-billed Grosbeak *(Eophona migratoria)* has a similar total mass of jaw muscle and generates a bite force of 36.1 N, which is high relative to its body mass (van der Meij & Bout 2004). Parrots seem to be less reliant on simple crushing of hard seeds favouring the use of the lower jaw and their feet to manipulate the food item between the more distal edge of the lower mandible, pushing the food item against the maxilla's palate, which is lined with ridges providing an uneven surface to chisel the seeds and nuts against, aiding in de-husking (Homberger 2003, Martens *et al*. 2013, Bright *et al*. 2019). Cranial kinesis is well developed in parrots (Homberger 2017) and the amounts and arrangement of muscles in the jaw apparatus may help contribute to the efficacy of this. The well-developed retractor muscles may help in the manipulation of food items between the mobile upper beak and the mandible.

Most muscles that are involved with closing the jaw in parrots exhibited positive allometry with body mass. These muscles were thin sheets with broad points of origin and/or insertion. The exception was the *ethmomandibularis*, which appeared to be composed of parallel fibres running between limited points of origin and insertion. If muscle mass is directly proportional to force generated by its contraction (Lieber & Ward 2011), and if the moment arms for the levers associated with jaw action are isometric, then larger parrots with more muscle mass will be able to generate a greater bite force than smaller parrots. This positive allometry has also been observed for total muscle mass in passerines (slope of 1.38) (Deeming *et al*. 2022) and in granivorous songbirds in particular (slope of 1.29) (van der Meij & Bout 2004). Species of the Fringillidae had significantly more jaw muscle mass than species of the Estrildidae (van der Meij & Bout 2004). By contrast, the slope of the relationship for non-passerine species was significantly negatively allometric and it may reflect a more functional aspect of the amounts of jaw muscle that individual species have. However, the analysis by Deeming *et al*. (2022) was limited in species range and only included data for two parrot species. Once bite forces are available for the parrots species described here it would be interesting to see how this changes the patterns described by Deeming *et al.* (2022).

Bite force in lizards has been shown to reflect tooth morphology and hence by association the diet with species dealing with harder food items having the stronger bite force (Jenkins & Shaw 2020). Both granivorous passerines and parrots have diets that include potentially hard seeds and nuts that require greater force to process compared with other food items, such as flesh. To date, only the Monk Parakeet (Carril *et al*. 2015) and the African Grey Parrot (Cost *et al*. 2020) have been studied but bite forces do seem to be relatively high compared to other bird species with comparable body mass. For instance, the Cooper's Hawk *(Accipiter cooperii)*, a bird of prey (Accipitriformes) of a similar size (360 g) to the African Grey Parrot (333 g, Dunning 2008), has a bite force of only 2–3 N (Sustaita & Hertel 2010) compared to the calculated bite force of 63 N for the parrot (Cost *et al*. 2020). The Monk Parakeet, which weighs less than half the mass of the Cooper's Hawk, has an estimated bite force of 16 N (Carril *et al*. 2015). Hawks kill their prey with the talons and use their beaks to tear their prey apart (Sustaita & Hertel 2010) so appear to have no need for a higher bite force, although falcons Falconiformes often kill their prey by biting (Pecsics *et al.* 2019). It is anticipated that calculated bite forces in the parrot species investigated here are also going to be high relative to body mass. Diet may, therefore, be a crucial aspect of defining the relationship between body mass and jaw muscle mass in birds. More research, from a much large dataset from a greater diversity of species, is required to explore the the more functional aspects of the jaw musclature in birds.

By contrast to body mass, the relationship between skull length and individual muscle mass in parrots was isometric in most muscle types, with one exception. Previously unreported, this relationship may reflect the physical limitations for muscle orgin offered by the skull. Bigger parrots need to accommodate more muscle in order to generate a greater bite force and it seems that this is simply achieved by increasing the size of the skull. It is unclear whether this also applies for other species of bird within, or across, orders and is worthy of further investigation. The exception in parrots was the *pterygoideus dorsalis*, which exhibited positive allometry with skull length. This adductor muscle originates on the surface of the palatine bone, which has rotated through 90 degrees and points downwards (Zusi 1993, Homberger 2003, 2017, Carril *et al*. 2015, Pecsics *et al.* 2020). This change in skull morphology appears to have two consequences. The first is that there is a large area of bone for the origin of the muscle and secondly, the distance between the origin and the insertion on the mandible is reduced. Muscle architecture is important in generating force, as the arrangement of the fibres relative to the central axis is a major determinant in how much of the force generated will be transferred efficiently (Lieber & Ward 2011). Shorter muscle fibres can generate higher forces (Biewener & Patek 2018) so this shortening of the *pterygoideus dorsalis* muscle may help increase the amount of force it can generate.

This study demonstrated that the mass of the different muscle types in the jaw apparatus of parrots varies between species. There is some suggestion that this will also be observed in other birds and is worthy of further investigation. To date the strongest bite force in birds has been calculated at 430 N for the Ostrich (*Struthio camelus*; Struthionidae, Struthioniformes) which has a jaw muscle mass of 16.9 g (Gussekloo & Bout 2005). However, the Large Ground Finch (*Geospiza magnirostris*; Thraupidae, Passeriformes) has only 0.664 g of jaw muscle and generates a bite force of 70.8 N (Herrel *et al.* 2005). Relative to body mass this is a bite

force of 2.16 N g^{-1}, over 500 times greater than that of the Ostrich (0.0043 N·g^{-1}). However, the Monk Parraket has a jaw muscle mass of 0.92 g but Carril *et al.* (2015) calculated its bite force at only 16 N (0.13 N g^{-1}). The Red-and-green Macaw studied here has a total muscle mass of almost 12 g (~1% of body mass) and so given the relationship between jaw muscle mass and bite reported by Deeming *et al.* (2022), it is predicted that it will have a bite force of 150 N (0.12 N g^{-1}). Given the well-muscled jaw apparatus of this large parrot, and the damage a parrot bite can inflict (King *et al*. 2015), these estimates seem rather low. Although bite force is generally low in birds (Deeming *et al*. 2022) compared to some reptiles (see Deeming 2022), our understanding of this relationship is based on a very relatively small dataset for a limited range of bird species. Moreover, in parrots an increase in bite force seems to be associated with an increase in skull size to accommodate more muscles. It is unknown whether this pattern is applicable to other birds within specific orders or even across birds as a whole. If we are going to be able to understand the evolutionary pressures on beak morphology (Hrabar & Perrin 2002, Bright *et al*. 2016, Cooney *et al*. 2017, Navalón *et al.* 2019) there will need to be further investigation into the allometry of the morphological and functional properties of the jaw musculature in a wider range of species.

Acknowledgements

We are grateful to Mr Steve Nichols and Miss Jess Newton at the Lincolnshire Wildlife Park Inc., The National Parrot Sanctuary, Friskney, Lincolnshire for donating their deceased parrots for use in this study. We are very grateful to the technical staff, in particular Marco Perez Tanchez, who helped immensely with the preparation of the skulls. Many thanks to Carl Soulsbury for his help with the statistical analysis. GPS is grateful to the UK Medical Research Council for funding (MR/T046619/1) as part of the NSF/CIHR/DFG/FRQ/UKRI-MRC Next Generation Networks for Neuroscience Program, and to the Royal Society for funding (UF120507).

References

Anderson, R. A., McBrayer, L. D. & Herrel, A. 2008. Bite force in vertebrates: opportunities and caveats for use of a nonpareil whole-animal performance measure. – Biological Journal of the Linnean Society 93: 709–720. DOI: 10.1111/j.1095-8312.2007.00905.x

Auersperg, A. M. I., Szabo, B., Von Bayern, A. M. P. & Kacelnik, A. 2012. Spontaneous innovation in tool manufacture and use in a Goffin's Cockatoo. – Current Biology 22(21): R903–R904. DOI: 10.1016/j.cub.2012.09.002

Bailey, N. T. J. 1981. Statistical Methods in Biology, 2nd ed. – Hodder and Stoughton, London

Bhattacharyya, B. N. 2013. Avian jaw function: adaptation of the seven-muscle system and a review. – Proceedings of the Zoological Society 66(2): 675–685. DOI: 10.1007/s12595-012-0056-x

Biewener, A. A. & Patek, S. N. 2018. Animal Locomotion. – Oxford University Press, Oxford

Bright, J. A., Marugán-Lobón, J., Rayfield, E. J. & Cobb, S. N. 2019. The multifactorial nature of beak and skull shape evolution in parrots and cockatoos (Psittaciformes). – BMC Evolutionary Biology 19: 104. DOI: 10.1186/s12862-019-1432-1

Bright, J. A., Marugán-Lobón, J., Cobb, S. N. & Rayfield, E. J. 2016. The shapes of bird beaks are highly controlled by nondietary factors. – Proceedings of the National Academy of Sciences of the United States of America 113(19): 5352–5357. DOI: 10.1073/pnas.1602683113

Bühler, P. 1981. Functional anatomy of the avian jaw apparatus. – In: King, A. S. & McClelland, J. (eds.) Form and Function in Birds, Vol. 2. – Academic Press, London, pp. 439–468.

Burger, A. E. 1978. Functional anatomy of the feeding apparatus of four South African cormorants. – Zoologica Africana 13(1): 81–102. DOI: 10.1080/00445096.1978.11447608

Burton, P. J. K. 1974a Feeding and the Feeding Apparatus in Waders. – British Museum, London

Burton, P. J. K. 1974b Jaw and tongue features of the Psittaciformes and other orders with special reference to the anatomy of the Tooth-billed Pigeon copy. – Journal of Zoology London 174(2): 255–276. DOI: 10.1111/j.1469-7998.1974.tb03156.x

Carril, J., Degrange, F. J. & Tambussi, C. P. 2015. Jaw myology and bite force of the Monk Parakeet (Aves, Psittaciformes). – Journal of Anatomy 227(1): 34–44. DOI: 10.1111/joa.12330

Cooney, C. R., Bright, J. A., Capp, E. J. R., Chira, A. M., Hughes, E. C., Moody, C. J. A. & Thomas, G. H. 2017. Mega-evolutionary dynamics of the adaptive radiation of birds. – Nature 542: 344–347. DOI: 10.1038/nature21074

Cost, I. N., Middleton, K. M., Sellers, K. C., Echols, M. S., Witmer, L. M., Davis, J. L. & Holliday, C. M. 2020. Palatal biomechanics and its significance for cranial kinesis in *Tyrannosaurus rex*. – Anatomical Record 303(4): 999–1017. DOI: 10.1002/ar.24219

Deeming, D. C. 2022. Inter-relationships among body mass, body dimensions, jaw musculature and bite force in reptiles. – Journal of Zoology 318: 23–33. DOI: 10.1111/jzo.12981

Deeming, D. C., Harrison, S. L. & Sutton, G. P. 2022. Inter-relationships among body mass, jaw musculature and bite force in birds. – Journal of Zoology 317(2): 129–137. DOI: 10.1111/jzo.12966.

Dunning, Jr., J. B. 2008. CRC handbook of avian body masses, 2nd ed. – CRC, Boca Raton, Florida

Freckleton, R. P., Harvey, P. H. & Pagel, M. 2002. Phylogenetic analysis and comparative data: a test and review of evidence. – American Naturalist 160(6): 712–726. DOI: 10.1086/343873

Genz, A. & Bretz, F. 2009. Computation of Multivariate Normal and t Probabilities, Series Lecture Notes in Statistics. – Springer-Verlag, Cham, Switzerland

Goodman, D. C. & Fisher, H. I. 1962. Functional Anatomy of the Feeding Apparatus in Waterfowl. – Southern Illinois Press

Gussekloo, S. W. S. & Bout, R. D. 2005. Cranial kinesis in palaeognathous birds. – Journal of Experimental Biology 208(17): 3409–3419. DOI: 10.1242/jeb.01768

Herrel, A., Spithoven, L., Van Damme, R. & De Vree, F. 1999. Sexual dimorphism of head size in *Gallotia galloti*: testing the niche divergence hypothesis by functional analyses. – Functional Ecology 13(3): 289–297. DOI: 10.1046/j.1365-2435.1999.00305.x

Herrel, A., Soons, J., Huber, S. K. & Hendry, A. P. 2005. Evolution of bite force in Darwin's finches: a key role for head width. – Journal of Evolutionary Biology 18(3): 669–675. DOI: 10.1111/j.1420-9101.2004.00857.x

Homberger, D. G. 2003. The comparative biomechanics of a prey-predator relationship: The adaptive morphologies of the feeding apparatus of Australian Black-cockatoos and their foods as a basis for the reconstruction of the evolutionary history of the Psittaciformes. – In: Bels, V. L., Gasc, J-P. & Casinos, A. (eds.) Vertebrate Biomechanics and Evolution. – BIOS Scientific Publishers Ltd., Oxford, pp. 203–228.

Homberger, D. G. 2017.The avian lingual and laryngeal apparatus within the context of the head and jaw apparatus, with comparisons to the mammalian condition: functional morphology and biomechanics of evaporative cooling, feeding, drinking, and vocalisation. – In: Maina, J. N. (ed.) The Biology of the Avian Respiratory System. – Springer, Cham, Switzerland, pp. 27–97. DOI: 10.1007/978-3-319-44153-5_2

Hrabar, H. D. K. & Perrin, M. 2002. The effect of bill structure on seed selection by granivorous birds. – African Zoology 37(1): 67–80. DOI: 10.1080/15627020.2002.11657157

Hull, C. 1991. A comparison of the morphology of the feeding apparatus in the Peregrine Falcon *Falco peregrinus*, and the Brown Falcon, *F. berigora* (Falconiformes). – Australian Journal of Zoology 39(1): 67–76. DOI: 10.1071/ZO9910067

Hull, C. 1993. Prey dismantling techniques of the Peregrine Falcon *Falco peregrinus* and the Brown Falcon *F. berigora*: their relevance to optimal foraging theory. – In: Olsen, P. (ed.) Australian Raptor Studies. – Australian Raptor Association, R.A.O.U., Sydney, pp. 330–336.

Jenkins, K. M. & Shaw, J. O. 2020. Bite force data suggests relationship between acrodont tooth implantation and strong bite force. – PeerJ 8: e9468. DOI: 10.7717/peerj.9468

Jetz, W., Thomas, G. H., Joy, J. B., Hartmann, K. & Mooers, A. O. 2012. The global diversity of birds in space and time. – Nature 491: 444–448. DOI: 10.1038/nature11631

King, I. C. C., Freeman, H. & Wokes, J. E. 2015. Managing parrot bite injuries to the hand: not just another animal bite. – Hand 10(1): 128–130. DOI: 10.1007/s11552-014-9644-8

Lieber, R. L. & Ward, S. R. 2011. Skeletal muscle design to meet functional demands. – Philosophical Transactions of the Royal Society B: Biological Sciences 366(1570): 1466–1476. DOI: 10.1098/rstb.2010.0316

Maestri, R., Patterson, B. D., Fornel, R., Monteiro, L. R. & de Freitas, T. R. O. 2016. Diet, bite force and skull morphology in the generalist rodent morphotype. – Journal of Evolutionary Biology 29(11): 2191–2204. DOI: 10.1111/jeb.12937

Martens, J., Hoppe, D. & Woog, F. 2013. Diet and feeding behaviour of naturalised Amazon Parrots in a European city. – Ardea 101(1): 71–76. DOI: 10.5253/078.101.0111

Navalón, G., Bright, J. A., Marugán-Lobón, J. & Rayfield, E. J. 2019. The evolutionary relationship among beak shape, mechanical advantage, and feeding ecology in modern birds. – Evolution 73(3): 422–435. DOI: 10.1111/evo.13655

Nogueira, M. R., Peracchi, A. L. & Monteiro, L. R. 2009. Morphological correlates of bite force and diet in the skull and mandible of phyllostomid bats. – Functional Ecology 23(4): 715–723. DOI: 10.1111/j.1365-2435.2009.01549.x

Paradis, E., Claude, J. & Strimmer, K. 2004. APE: analyses of phylogenetics and evolution in R language. – Bioinformatics 20(2): 289–290. DOI: 10.1093/bioinformatics/btg412

Pecsics, T., Laczi, M., Nagy, G., Kondor, T. & Csörgő, T. 2019. Analysis of skull morphometric characters in diurnal raptors (Accipitriformes and Falconiformes). – Ornis Hungarica 27(1): 117–131. DOI: 10.2478/ orhu-2019-0008

Pecsics, T., Laczi, M., Nagy, G. & Csörgő, T. 2020. Skull morphometric characters in parrots (Psittaciformes). – Ornis Hungarica 28(1): 104–120. DOI: 10.2478/orhu-2020-0008

Provost, K. L., Joseph, L. & Tilston Smith, B. 2018. Resolving a phylogenetic hypothesis for parrots: implications from systematics to conservation. – Emu – Austral Ornithology 118(1): 7–21. DOI: 10.1080/01584197.2017.1387030

R Development Core Team 2021. R: A language and environment for statistical computing. – R Foundation for Statistical Computing

Sakamoto, M. 2021. Assessing bite force estimates in extinct mammals and archosaurs using phylogenetic predictions. – Palaeontology 64(5): 743–753. DOI: 10.1111/pala.12567

Sims, R. 1955. The morphology of the head of the Hawfinch *(Coccothraustes coccothraustes)*. – Bulletin of the British Museum (Natural History) Zoology 2: 371–393.

Soons, J., Genbrugge, A., Podos, J., Adriaens, D., Aerts, P., Dirckx, J. & Herrel, A. 2015. Is beak morphology in Darwin's finches tune to loading demands? – PLoS One 10(6): e0129479. DOI: 10.1371/journal.pone.0129479

Soons, J., Herrel, A., Genbrugge, A., Adriaens, D., Aerts, P. & Dirckx, J. 2012. Multi-layered bird beaks: a finite-element approach towards the role of keratin in stress dissipation. – Journal of the Royal Society Interface 9(73): 1787–1796. DOI: 10.1098/rsif.2011.0910

Sustaita, D. 2008. Musculoskeletal underpinnings to differences in killing behavior between North American accipiters (Falconiformes: Accipitridae) and falcons (Falconidae). – Journal of Morphology 269(3): 283–301. DOI: 10.1002/jmor.10577

Sustaita, D. & Hertel, F. 2010. In vivo bite and grip forces, morphology and prey-killing behavior of North American accipiters (Accipitridae) and falcons (Falconidae). – Journal of Experimental Biology 213(15): 2617–2628. DOI: 10.1242/jeb.041731

Toft, C. A. & Wright, T. F. 2015. Parrots of the Wild. A Natural History of the World's Most Captivating Birds. – University of California Press, Oakland

Tokita, M. 2003. The skull development of parrots with special reference to the emergence of a morphologically unique cranio-facial hinge. – Zoological Science 20(6): 749–758. DOI: 10.2108/zsj.20.749

van Der Meij, M. A. A. & Bout, R. G. 2004. Scaling of jaw muscle size and maximal bite force in finches. – Journal of Experimental Biology 207(16): 2745–2753. DOI: 10.1242/jeb.01091

van der Meij, M. A. A. & Bout, R. G. 2006. Seed husking time and maximal bite force in finches. – Journal of Experimental Biology 209(17): 3329–3335. DOI: 10.1242/jeb.02379

Venables, W. N. & Ripley, B. D. 2002. Modern Applied Statistics with S, 4th ed. – Springer, New York

Verma, T. P., Kumathalli, K. I., Jain, V. & Kumar, R. 2017. Bite force recording devices – A review. – Journal of Clinical and Diagnostic Research 11(9): ZE01–ZE05. DOI: 10.7860/JCDR/2017/27379.10450

Wang, H., Yan, J. & Zhang, Z. 2017. Sexual dimorphism in jaw muscles of the Japanese Sparrowhawk *(Accipiter gularis)*. – Anatomy, Histology and Embryology 46(6): 558–562. DOI: 10.1111/ahe.12309

Warton, D. I. & Hui, F. K. C. 2011. The arcsine is asinine: the analysis of proportions in ecology. – Ecology 92(1): 3–10. DOI: 10.1890/10-0340.1

Zusi, R. L. 1993. Patterns of diversity in the avian skull. – In: Hanken, J. & Hall, B. K. (eds.) The Skull, Vol. 2.: Patterns of Structural and Systematic Diversity. – The University of Chicago Press, Chicago, pp. 391–437.